

THERMAL ISOCREEP CURVES OBTAINED DURING MULTI-AXIAL CREEP TESTS ON RECRYSTALLIZED ZIRCALOY-4 AND M5TM ALLOY

M. Rautenberg^{1,2}, D. Poquillon², P. Pilvin³, C. Grosjean^{1,2}, J.M. Cloué¹, X. Feaugas⁴

¹ AREVA, AREVA NP, 10, rue Juliette Récamier, 69456 Lyon, FRANCE

² CIRIMAT, CNRS/UPS/INPT, 4 allée Emile Monso, 31030 Toulouse, FRANCE

³ LIMATB, Univ. Bretagne-Sud, rue de Saint-Maudé, 56321 Lorient, FRANCE

⁴ LEMMA, Université de La Rochelle, avenue Michel Crépeau, 17042 La Rochelle, FRANCE

E-mail of corresponding author: mrautenb@gmail.com

ABSTRACT

Zirconium alloys are widely used in the nuclear industry. Several components, such as cladding or guide tubes, undergo strong mechanical loading during and after their use inside the pressurized water reactors. The current requirements on higher fuel performances lead to the developing on new Zr based alloys exhibiting better mechanical properties. In this framework, the creep behaviors of recrystallized Zircaloy-4 and M5TM, have been investigated and then compared. In order to give a better understanding of the thermal creep anisotropy of the Zr-based alloys, multi-axial creep tests have been carried out at 673K. Using a specific device, creep conditions have been set using different values of $\beta = \sigma_{zz} / \sigma_{\theta\theta}$, σ_{zz} and $\sigma_{\theta\theta}$ being respectively the axial and hoop creep stresses. Both axial and hoop strains are measured during each test which is carried out until stationary creep is stabilized. The steady-state strain rates are then used to build isocrep curves.

Considering the isocrep curves, the M5TM alloy shows a largely improved creep resistance compared to the recrystallized Zircaloy-4, especially for tubes under high hoop loadings ($0 < \beta < 1$). The isocrep curves are then compared with simulations performed using two different mechanical models. Model 1 uses a von Mises yield criterion, the model 2 is based on a Hill yield criterion. For both models, a coefficient derived from Norton law is used to assess the stress dependence.

INTRODUCTION

Zirconium alloys are widely used in nuclear applications, and more specifically in the production of fuel rod cladding tubes. In service, these components are subjected to complex thermo-mechanical loadings but also to other solicitations (irradiation, corrosion...). In order to improve the design and the lifetime of such structures, mechanical models have been developed. Therefore, to fit the model to reality, testing creep behavior of fuel claddings is essential. The creep anisotropy of these components is well known [1] and mainly due to the cold pilgering rolling process used to form the tubes and inducing an anisotropic crystallographic texture in the polycrystalline material. Polycrystalline models dedicated to Zirconium alloys have been developed [2-4], taking into account the specific distribution of grain orientations which is optimized in cladding tubes because of its strong influence on the mechanical behavior [5, 6]. The accuracy of these models was observed for zirconium alloys by several authors [7-9]. However, they are not yet used for design applications, as the computation time would be too important. In the future, polycrystalline models could nevertheless be considered as a virtual creep testing device, whose results could be used to build simplified models. The most suitable models may be chosen by comparison with experimental results. In a previous study, creep test have been carried out on recrystallized Zircaloy-4 and M5TM [10-12] with multiaxial loadings at 673K. During these experiments, strain evolutions were measured both in the axial and hoop directions to allow a 3-D characterization of the creep anisotropy.

The aim of the present paper is to compare two simplified models using an isotropic or an anisotropic formulation of the equivalent applied stress. Their ability to fit experimental data is presented for both investigated alloys. Thus, in the first part of this paper, we will detail the material and the device used for the creep tests. Then the experimental results and the tested models will be presented.

MATERIALS, EXPERIMENTAL DEVICE AND CREEP TESTS

The investigated zirconium alloys are recrystallized Zircaloy-4 and M5TM. The device used (CAT.0 for Creep Advanced Testing) have been especially developed for multiaxial tests on tubes [10-12]. It allows an axial load up to 5 kN and an internal pressure up to 200 bars. The axial and hoop strains are measured by laser

extensometers located in front of the small quartz windows of a radiative furnace that surrounds the tested sample. The specimens are 130 mm long segments of tubes. They present an outer diameter between 9.5 mm and 11.5mm and a thickness between 0.5mm and 0.6mm. All the tubes were formed by a cold pilgering rolling process and were then subjected to a recrystallisation heat treatment, resulting in a fully recrystallized hexagonal close packed microstructure. This cold-working forming process induces anisotropic crystallographic textures which are comparable for both investigated alloys. C-axes of the grains are mainly orientated around $\pm 30^\circ$ of the radial direction resulting in a mechanical anisotropy [12, 13].

Table 1: Chemical compositions.

	Sn	Fe	Cr	O	Nb	Zr
recrystallized Zircaloy-4	1.29 wt%	0.22 wt%	0.12 wt%	0.12 wt%		Bal.
M5 TM	<50 ppm	< 400ppm	<50 ppm	0.146 wt%	1 wt%	Bal.

All the tests were realized at a temperature of 673K. Creep tests were stopped when stationary creep strain rate was stabilized. Table 2 shows the different stress levels used for the present study, in order to scan different biaxiality ratios $\beta = \sigma_{zz}/\sigma_{\theta\theta}$, σ_{zz} and $\sigma_{\theta\theta}$ being respectively the axial and hoop creep stresses. Stresses are normalized with a division by σ_i , the applied axial stress for a measured equivalent strain rate of $3.5 \times 10^{-8} \text{ s}^{-1}$, with a hoop stress set to zero on the M5TM alloy.

Table 2: Applied hoop and axial creep stresses for the experimental data used to build the models.

β	M5 TM		recrystallized Zircaloy-4	
	$\sigma_{\theta\theta}/\sigma_i$	σ_{zz}/σ_i	$\sigma_{\theta\theta}/\sigma_i$	σ_{zz}/σ_i
∞	0	0.75	0.00	0.83
	0	0.93		
	0	1.04		
$-\infty$	0	-0.83		
	0	-1.04		
3	0.42	1.25		
2.65	0.35	0.93	0.43	1.13
1.5	1	1.50	0.92	1.38
1	1.28	1.28	1.30	1.28
	1.42	1.42		
0.75	1.10	0.83	1.27	0.94
	1.45	1.09		
0.5	1.25	0.63	1.25	0.63
0	1.25	0	1.25	0

A SIMPLIFIED MACROSCOPIC MODELING OF CREEP BEHAVIOR

A partition of the elastic and viscoplastic strain is used:

$$\underline{\underline{\varepsilon}} = \underline{\underline{\varepsilon}}^e + \underline{\underline{\varepsilon}}^p \quad (1)$$

$$\overline{\sigma} = \overline{C} \overline{\varepsilon}^e = \overline{C} (\overline{\varepsilon} - \overline{\varepsilon}^P) \quad (2)$$

where \overline{C} is the Hooke tensor of the material. If the yield stress of the proposed model is anisotropic, the elastic part of the behavior will be supposed isotropic. Thus, using tensorial notations:

$$\overline{\varepsilon} = \begin{pmatrix} \varepsilon_{11} \\ \varepsilon_{22} \\ \varepsilon_{33} \\ \varepsilon_{12} \\ \varepsilon_{23} \\ \varepsilon_{13} \end{pmatrix} = \begin{pmatrix} \varepsilon_{11}^e \\ \varepsilon_{22}^e \\ \varepsilon_{33}^e \\ \varepsilon_{12}^e \\ \varepsilon_{23}^e \\ \varepsilon_{13}^e \end{pmatrix} + \begin{pmatrix} \varepsilon_{11}^P \\ \varepsilon_{22}^P \\ \varepsilon_{33}^P \\ \varepsilon_{12}^P \\ \varepsilon_{23}^P \\ \varepsilon_{13}^P \end{pmatrix} \quad \text{and} \quad \overline{C} = \begin{pmatrix} C_{11} & C_{12} & C_{12} & & & \\ C_{12} & C_{11} & C_{12} & & & \\ C_{12} & C_{12} & C_{11} & & & \\ & & & C_{44} & & \\ & & & & C_{44} & \\ & & & & & C_{44} \end{pmatrix} \quad (3)$$

The coefficient of \overline{C} can easily be deduced from the Young modulus E, the Poisson's ratio ν and the shear modulus G:

$$C_{44} = G ; C_{12} = \frac{\nu C_{44}}{1-2\nu} = \frac{\nu G}{1-2\nu} ; C_{11} = C_{12} + C_{44} \quad (4)$$

The dislocation density ρ_s for each slip system s is defined as followed:

$$\frac{d\rho_s}{dt} = \frac{|\dot{\gamma}_s|}{b} \left(\frac{1}{L} - 2Y_s \rho_s \right) - B(\rho_s - \rho_0)^2 \quad (5)$$

Where b is the Burgers vector, L is the mean free path length of dislocations, Y_s the annihilation distance, ρ_s the dislocation density for the system s [8, 13], and $\dot{\gamma}_s$ its corresponding strain rate.

As the simplified model used does not discretize activated slip systems, the expression for the global dislocation density ρ is similar to Eq. (5):

$$\frac{d\rho}{dt} = \frac{1}{b} \times \frac{d|\varepsilon^P|}{dt} \left(\frac{1}{L} - 2Y_a \rho \right) - B(\rho - \rho_0)^2 \quad (6)$$

Where Y_a stands for an average of the different Y_s and ε^P is the equivalent plastic strain.

The evolution of work hardening R proposed is the following:

$$R = \sigma_0 + \alpha G b \sqrt{\rho} \quad (7)$$

where σ_0 corresponds to an initial yield strength and α to a hardening coefficient. Considering the activated slip systems in hexagonal close packed zirconium during creep at 673K, the burgers vector b can be taken as the lattice parameter <a> [13].

To get dimensionless expressions from Eq. (6), a new internal variable $q = b^2 \rho$ is introduced, and the equation is then:

$$\frac{dq}{dt} = \frac{d|\varepsilon_{zz}^P|}{dt} \left(\frac{b}{L} - \frac{2Y_a}{b} q \right) - \frac{B}{b^2} (q - q_0)^2 \quad (8)$$

$$\text{with } R = \sigma_0 + \alpha G \sqrt{q} \quad (9)$$

If p is the cumulated viscoplastic strain, its rate is given by \dot{p} :

$$\dot{p} = \sqrt{\frac{2}{3} \overline{\dot{\varepsilon}^P} : \overline{\dot{\varepsilon}^P}} \quad (10)$$

In order to model multiaxial loadings, a simplified anisotropic model is proposed using a Hill criterion H_2 for viscoplastic flow as detailed in equations 11 and 12.

$$F(\overline{\sigma}, R) = H_2(\overline{\sigma}) - R \quad (11)$$

$$\text{with } H_2(\overline{\sigma}) = \sqrt{H_r(\sigma_{\theta\theta} - \sigma_{zz})^2 + H_\theta(\sigma_{zz} - \sigma_{rr})^2 + H_z(\sigma_{rr} - \sigma_{\theta\theta})^2} \quad (12)$$

Assuming that for pure axial loading (when $\sigma_{\theta\theta}$ et σ_{rr} are set to 0), plastic flow occurs for $\sigma_{zz} = \sigma_0$, then using Eq. (7), (11) and (12) we get a relation between H_r and H_θ :

$$H_\theta = 1 - H_r \quad (13)$$

For an isotopic behaviour $H_r = H_z$ and, as a consequence, in that particular case $H_r = H_z = H_\theta = 0.5$ and equation 12 becomes the definition of the Von Mises criterion.

For the viscoplastic flow, the normality rule leads to:

$$\frac{d\overline{\varepsilon}^P}{dt} = \left(\frac{F}{K}\right)^n \frac{\partial F}{\partial \overline{\sigma}} \quad \text{if } F > 0 \quad (14)$$

So if $\overline{\sigma}$ stands for the stress and D stands for the deviator operator then:

$$\frac{d\overline{\varepsilon}^P}{dt} = \frac{3}{2} \left(\frac{F}{K}\right)^n \frac{D(\overline{\sigma})}{H_2(\overline{\sigma})} \quad (15)$$

To summarize, 10 different coefficients are used $\left\{E, \nu, n, K, \alpha, \frac{L}{b}, \frac{Y_a}{b}, \frac{B}{b^2}, H_r, H_z\right\}$. They can be reduced to 8 if

we set $H_r = H_z = 1/2$. Four experimental variables $\left\{\overline{\psi}, \overline{\sigma}, \overline{\varepsilon}, T\right\}$ are taken into account and three internal variables

$\left\{\overline{\varepsilon}^P; \dot{p}; q\right\}$ are computed during the calculations. For both materials, the software SIDOLO [14] was used to fit the

coefficients in order to minimize the difference between simulation and experimental data for axial and hoop strain. For all the simulations, the Young modulus and the Poisson's ratio were fixed to respectively 78000 MPa and 0.37.

The first run of simulations was carried out with $H_r = H_z = H_\theta = 0.5$. This "model 1" corresponds to the classical Von Mises isotropic criterion. The 6 remaining coefficients were identified on axial creep tests.

For the second run of simulations H_r and H_z were taken as free coefficients. This "model 2" corresponds to a Hill approach. The 8 coefficients of this model were identified using all the tests (axial and multiaxial creep tests).

RESULTS

The optimizations which minimize the difference between simulated and experimental creep strain curves were carried out for both alloys and for both models.

Table 3: Value of models coefficient after identification using the data base of table 1

Coefficients	M5 [®]	M5 [®]	recrystallized Zircaloy-4	recrystallized Zircaloy-4
	Model 1 (Von Mises)	Model 2 (Hill)	Model 1 (Von Mises)	Model 2 (Hill)
E (MPa) (locked)	78000	78000	78000	78000
ν (locked)	0,37	0,37	0,37	0,37
n	5,83	5,62	5,84	5,97
K (MPa)	1644	1801	1647	1355
σ_0 (MPa)	1,31	1,32	1,35	1,32
α	0,63	0,627	0,35	0,615
L/b	2181	1827	1975	1834
Y_a/b	51,8	60,27	45,2	50,3
B/b^2 (s ⁻¹)	$0,42 \cdot 10^{-4}$	$0,35 \cdot 10^{-4}$	$0,37 \cdot 10^{-4}$	$0,42 \cdot 10^{-4}$
H_r	0,50 (locked)	0,514	0,50 (locked)	0,48
H_z	0,50 (locked)	0,368	0,50 (locked)	0,29

Table 3 details the values obtained at the end of the optimization process. The n exponent remains quite the same in any case. The initial yield strengths σ_0 are close to 0. Model 1 allows a good description of axial creep tests for both alloys (Fig. 1) but not for loadings in which the values of $\beta = \sigma_{zz}/\sigma_{\theta\theta}$ is lower than 2 (Fig. 2). Figure 1 shows that with similar axial loadings, the M5TM alloy exhibits a lower strain rate than the Zircaloy-4. This tendency is confirmed for all the tested loading directions.

Model 2 enables an anisotropic approach using Hill coefficients. We notice that this approach is more suitable as the optimization process leads to values of H_z that differs from 0.5. Furthermore, creep anisotropy seems enhanced for the recrystallized Zircaloy-4 compared with the M5TM alloy.

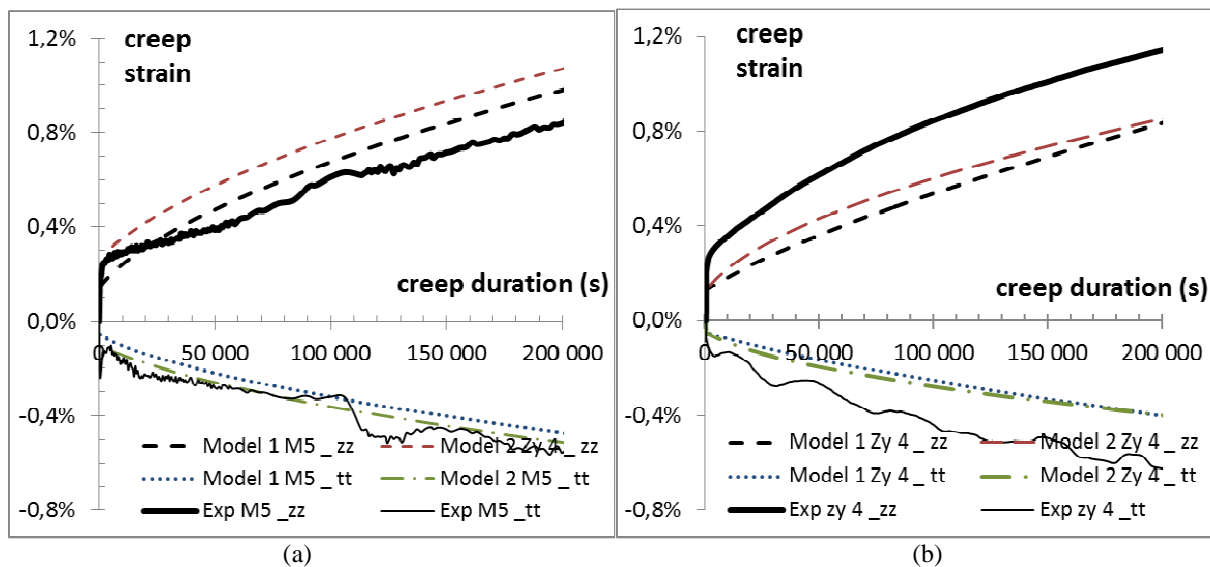


Fig. 1: Comparison between experimental data and models for axial creep tests. a) Recrystallized Zircaloy-4, $\sigma_{zz}/\sigma_i = 0.83$ b) M5TM, $\sigma_{zz}/\sigma_i = 0.93$.

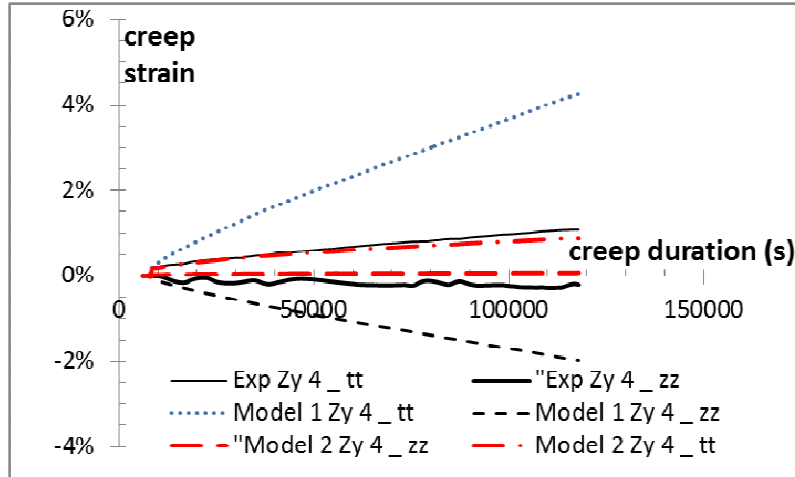


Fig. 2: Comparison of experimental data, model 1 and model 2 for recrystallized Zircaloy-4 crept at $\beta=0.5$: $\sigma_{\theta\theta}/\sigma_i = 1.25$; $\sigma_{zz}/\sigma_i = 0.63$

Using a large experimental data [15], it is possible to compute for each alloy and for each biaxiality ratio β a Norton coefficient n^{exp} . The experimental data can be then interpolated in order to determine “isocreep curves”, *i.e.* the locus $[\sigma_{\theta\theta}; \sigma_{zz}]$ for a constant secondary strain rate, which is calculated using Eq. (16) :

$$\frac{d\epsilon_{eq}}{dt} = \dot{p} = \sqrt{4/3[(\dot{\epsilon}_{\theta\theta})^2 + (\dot{\epsilon}_{zz})^2 + (\dot{\epsilon}_{\theta\theta})(\dot{\epsilon}_{zz})]} \quad \text{and} \quad \frac{d\epsilon_{eq}}{dt} = A(\sigma_{VonMises})^{n^{exp}} \quad (16)$$

Besides, simulations are carried out with models 1 and 2 to determine which stress levels leads to a given secondary creep strain rate of $3.5 \times 10^{-8} s^{-1}$ for each investigated biaxiality ratios. This enables the plot of isocreep curves that can be compared to those obtained with the interpolation of the experimental data. Examples of experimental and numerical isocreep curves are plotted in Fig. 3. Both models are not able to reproduce the creep tube resistance for stress biaxiality ratios between 2 and 0.5. But model 2 is, as expected, closer from the experimental data.

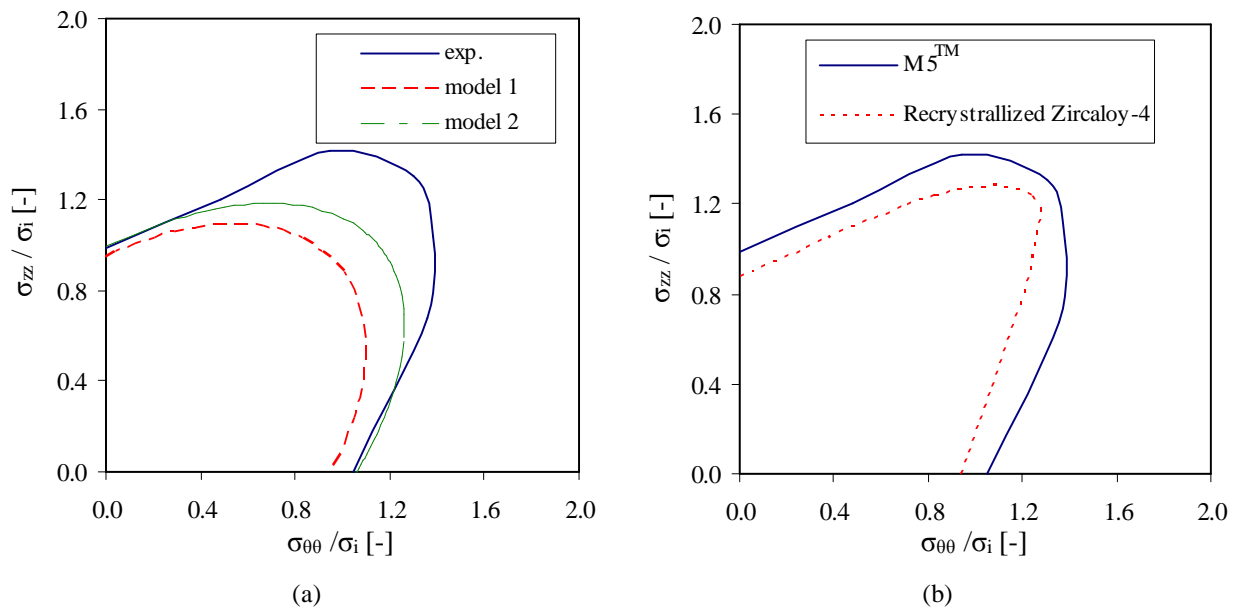


Fig. 3: Iso creep curves for an equivalent strain rate of $3.5 \times 10^{-8} s^{-1}$ at 673K. a) Isocreep curves obtained from model 1, model 2 and experimental data the M5TM alloy. b) Comparison between the investigated alloys.

Isocreep curves of both investigated alloys have also been compared. Results are plotted on Fig. 3b for a value of $3.5 \times 10^{-8} \text{ s}^{-1}$. The M5TM exhibits a better creep resistance than the recrystallized Zircaloy-4, especially for biaxiality ratios below 1.

CONCLUSION

The present experimental results constitute an evidence of the creep anisotropy of zirconium recrystallized alloys. Effectively, the global shapes of the isocreep curves differ from what can be obtained using an isotropic criterion (model 1). This could mean that anisotropic considerations are more suitable for an accurate modeling. Despite the use of an anisotropic Hill criterion, model 2 is still not able to fit the experimental data for $0.5 < \beta < 2$.

This region of the isocreep plot seems to exhibit a complex behavior that seems to be more alloy-dependant, as it is the only part of the iso-creep curve which has a different shape for the two considered alloys (Fig. 3b). The fact that a polycrystalline model could fit more easily the experimental creep strains and isocreep curves [16] can be interpreted in different ways. First, the higher number of considered parameters for this kind of model allows a better setting, on a multi-scale experimental data (crystallographic texture measurements, TEM observations, tensile tests,...). However, a major explanation for the accuracy of this approach is the discrimination of the different activated slip systems. It can enable the model to fit the variation from “hard” to “ductile” creep behaviors more easily. Thus, cross-slip or secondary slip systems can be activated in different proportions according to the direction of loading and its orientation towards the crystallographic texture.

The strongly heterogeneous crystallographic texture of the studied zirconium alloys, combined to the limited possibilities of slip systems, is the principal explanation for the shapes of the isocreep curves. In particular, the unusual curvatures for $0.5 < \beta < 2$ are linked to a significant evolution in the repartition of dislocation glide [17]. A similar explanation can be given to account for the linear evolution of the curves for $2 < \beta < \infty$ and $0 < \beta < 0.5$. And linear shapes, as well as “too convex” shapes, cannot be globally described with quadratic criterions such as those used in the models presented. We can therefore assume that macroscopic models using equivalent stresses calculated with a non-quadratic law, like the Hosford criterion [18], would allow an improved accuracy.

ACKNOWLEDGEMENTS

The authors are grateful to Dr. M. Priser for his contribution to the modeling, and to K. Niang (AREVA NP – CEZUS) who provided the tubes.

REFERENCES

- [1] Brachet, J.C., Béchade, J.L., Castaing, A., Le Blanc, L., Jouen, T., “Relationship between crystallographic texture and dilatometric behaviour of a hexagonal polycrystalline material”, *Materials Science Forum*, Vol. 529, 1998, pp. 273-275.
- [2] Miller, A K., “Unified constitutive equations for creep and plasticity”, Elsevier Applied Science, New York, 1987.
- [3] Brenner, R., “Influence de la microstructure sur le comportement en fluage thermique d'alliages de zirconium: analyse expérimentale et mise en oeuvre de méthodes d'homogénéisation”, Ph.D., Université Paris XIII, 2001.
- [4] Pilvin, P., “Approches multi-échelles pour la prévision du comportement anélastique des métaux”, Ph.D., Université Paris VI, 1990.
- [5] Delobelle, P., Robinet, P., Geyer, P., Bouffioux, P., “A model to describe the anisotropic viscoplastic behaviour of Zircaloy-4 tubes”, *Journal of Nuclear Materials*, Vol. 135, 1996, p. 238.
- [6] Priser, M., Cloué, J.M., Pilvin, P., Poquillon, D., “A mixed yield surface for modeling the anisotropic mechanical behavior of Zirconium alloy”, *20th International Conference on Structural Mechanics in Reactor Technology*. Helsinki, Finland, 2009.
- [7] Geyer, P., “Comportement élasto-viscoplastique de tubes en zircaloy 4 : approche expérimentale et modélisation micromécanique“, Ph.D., Ecole Nationale Supérieure des Mines de Paris, 1999.
- [8] Fandeur, O., Pilvin, P., Prioul, C., “Modélisation du comportement mécanique du Zircaloy-4“, *Journal de Physique IV*, Vol. 11, 2001.
- [9] Onimus, F., Béchade, J.-L., “A polycrystalline modeling of the mechanical behavior of neutron irradiated zirconium alloys“, *Journal of Nuclear Materials*, Vol. 384, 2008, pp. 163-174.

- [10] Grosjean, C., Poquillon, D., Salabura, J.-C., Cloué, J.-M., “Fuel rod testing in creep conditions under multiaxial loadings: A new device and experimental results”, *19th International Conference on Structural Mechanics in Reactor Technology*, Toronto, Canada, 2007.
- [11] Grosjean, C., Poquillon, D., Cloué, J.-M., “Innovative creep device and analysis method applied to cladding tubes in Zirconium alloys”, *2nd ECCC Conference-Creep & Fracture in High temperature Components-Design a life Assessment*, Dubendorf, Germany, 2009.
- [12] Grosjean, C., Poquillon, D., Salabura, J.-C., Cloué, J.-M., “Experimental creep behaviour determination of cladding tube materials under multiaxial loadings”, *Materials Science and Engineering A*, Vol. 510-511, 2009, pp. 332-336.
- [13] Priser, M., Rautenberg, M., Cloué, J.-M., Pilvin, Ph., Feaugas, X., Poquillon, D., “Micromechanical approach of visco-plastic behavior of recrystallized zircaloy-4”; *Journal of ASTM International*, Vol. 8, 2011, pp. 10-29.
- [14] Cailletaud, G., Pilvin, Ph., “Identification and Inverse problems: a modular approach”, *American Society of Mechanical Engineers*, Vol. 33, 1993, p.43.
- [15] Grosjean, C., “Anisotropie de comportement en fluage thermique de tubes gaine et de tubes guide en alliages de Zirconium. Développement expérimentaux et résultats”, Ph.D., Université de Toulouse, 2009.
- [16] Priser, M., “Analyses multi-échelles du comportement en fluage d’alliages de Zirconium.”, Ph.D., Université de Bretagne-Sud, 2011.
- [17] Geyer, P., Feaugas, X., Pilvin, Ph., “Modelling of the anisotropic viscoplastic behavior of fully annealed Zircaloy-4 tubes by a polycrystalline model”, *Plasticity’99*, Cancun, Mexico, 1999, pp.133-136.
- [18] Hosford, W.F., “A generalised isotropic yield criterion”, *Journal of Applied Mechanics*, Vol. 39, 1972, pp.607-609.